Article

Limited Variations in N CSA Magnitudes and Orientations in Ubiquitin Are Revealed by Joint Analysis of Longitudinal and Transverse NMR Relaxation

Peter Damberg, Jri Jarvet, and Astrid Grslund

J. Am. Chem. Soc., **2005**, 127 (6), 1995-2005• DOI: 10.1021/ja045956e • Publication Date (Web): 21 January 2005

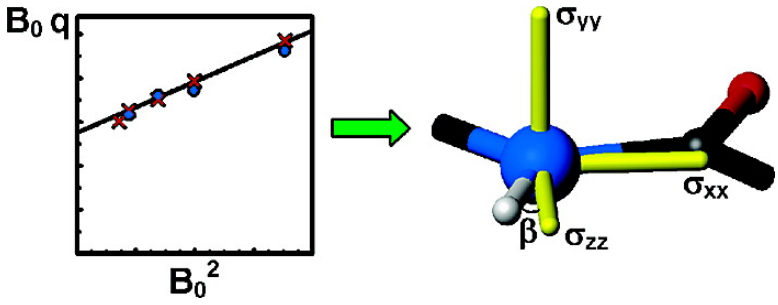

More About This Article

Additional resources and features associated with this article are available within the HTML version:

- Supporting Information
- Links to the 3 articles that cite this article, as of the time of this article download
- Access to high resolution figures
- Links to articles and content related to this article
- Copyright permission to reproduce figures and/or text from this article

View the Full Text HTML

J|A|C|S
ARTICLES
Published on Web 01/21/2005

Limited Variations in ^{15}N CSA Magnitudes and Orientations in Ubiquitin Are Revealed by Joint Analysis of Longitudinal and Transverse NMR Relaxation

Peter Damberg,* Jüri Jarvet, and Astrid Gräslund

Contribution from the Department of Biochemistry and Biophysics, Stockholm University, Svante Arrhenius v.12, S-106 91, Sweden

Received July 7, 2004; E-mail: peter.damberg@dbb.su.se

Abstract: The site-specific magnitudes and orientations of the chemical shift tensors have been estimated for 70 backbone ^{15}N-nuclei in human ubiquitin from the field dependence of dynamic independent ratios between relaxation rates, both longitudinal and transverse, measured at 9.4, 11.7, 14.1, and 18.8 T. The results were jointly analyzed with previously published relaxation data [Fushman; Tjandra; Cowburn. *J. Am. Chem. Soc.* **1998**, *120*, 10947−10952] [Kövér; Batta. *J. Mag. Reson.* **2001**, *150*, 137−146]. The effective magnitudes of the anisotropies distribute around 169 ppm with a variability of 5 ppm. The orientation factors, reflecting the orientation of the CSA relative to the NH bond, distribute around −0.80 with a variability of 0.04, which corresponds to an angle between the symmetry axis of an assumed axially symmetric shielding tensor and the NH bond of 21.4°, and a variability of 2.3°. Correlations with the isotropic ^{15}N-chemical shifts are observed. Variations in the shielding anisotropies add uncertainty to the obtained order parameters proportional to the square of the magnetic field, when data are analyzed using an assumed invariant CSA tensor for all sites. Around 3% additional uncertainty in the order parameters for 800 MHz data is expected. The optimal TROSY field for amide nitrogen TROSY is estimated, with only marginal variations due to site-to-site variations. Variations in the shielding tensors add uncertainty to the exchange terms calculated from cross-correlation rates. An approach for estimating the exchange terms is suggested, where the uncertainty due to CSA-variations is minimized.

Introduction

In NMR, the nuclear chemical shift tensor, which describes the shielding of a nuclear spin from the external magnetic field, carries important information about the local electronic environment of the nucleus. In principle the tensor has properties related to molecular structure. The anisotropy of the tensor (Chemical Shift Anisotropy, CSA) manifests itself as a relaxation mechanism additional to the dipole−dipole interaction.

Knowledge of the tensor is needed for the interpretation of NMR relaxation data to yield information on molecular dynamics. This is the case when nanosecond to picosecond dynamics are studied and also in approaches where the presence of millisecond to microsecond dynamics is detected by comparing the decay rate of transverse magnetization to the transverse CSA/dipole−dipole cross-correlation relaxation rate. Recently chemical shift changes upon weak alignment have been used as new constraints for structure refinement.[1] This procedure is limited by the knowledge of the site-specific shielding anisotropy, which further increases the interest for characterizing the variability in the shielding tensor. Application of so-called TROSY[2] techniques to increase the resolution of NMR spectra of large molecules depends on the interference between dipolar and CSA relaxation, i.e., the CSA/dipole−dipole cross-correlation, and the degree of cancellation between the two relaxation mechanisms depends on the orientation of the shielding tensor relative to the NH bond as well as their magnitudes.

Variations from site to site of the magnitude and the orientation of the CSA tensor is therefore also of interest when estimating the optimal magnetic field for TROSY and assessing the usefulness of the TROSY approach.

Solid state NMR has been the major method to obtain the components of the chemical shift tensors in powders or crystals of peptides. Such experiments require site-specific isotope labeling of the peptide and have, therefore, given only limited amounts of information, mainly on very short peptides. Recently, a number of high-resolution NMR methods based on relaxation measurement have become available for studies of protein chemical shift tensors,[3−9] such as for ^{15}N of the amide in the protein backbone. The high-resolution methods typically do not

(1) Lipsitz, R. S.; Tjandra, N. *J. Magn. Reson.* **2003**, *164*, 171−6.
(2) Pervushin, K.; Riek, R.; Wider, G.; Wüthrich, K. *Proc. Natl. Acad. Sci. U.S.A.* **1997**, *94*, 12366−71.
(3) Kroenke, C. D.; Rance, M.; Palmer, A. G. *J. Am. Chem. Soc.* **1999**, *121*, 10119−25.
(4) Kövér, K. E.; Batta, G. *J. Magn. Reson.* **2001**, *150*, 137−46.
(5) Fushman, D.; Tjandra, N.; Cowburn, D. *J. Am. Chem. Soc.* **1998**, *120*, 10947−52.
(6) Canet, D.; Barthe, P.; Mutzenhardt, P.; Roumestand, C. *J. Am. Chem. Soc.* **2001**, *123*, 4567−76.
(7) Boyd, J.; Redfield, C. *J. Am. Chem. Soc.* **1998**, *120*, 9692−3.
(8) Fushman, D.; Tjandra, N.; Cowburn, D. *J. Am. Chem. Soc.* **1999**, *121*, 8577−82.
(9) Damberg, P.; Jarvet, J.; Allard, P.; Gräslund, A. *J. Biomol. NMR* **1999**, *15*, 27−37.

give information on the full chemical shift tensors, but on the magnitude ($\Delta\sigma_{eff}$) of the chemical shift anisotropy (CSA) and, in some cases, on an orientation factor (f_{orient}). The orientation factor is dependent on the relative orientations of the two tensors describing the dipolar interactions and the CSA of the relaxing pair of nuclei. For two proteins the three principal components of the shielding tensor and their orientation relative to the peptide plane have been evaluated from the small chemical shift changes caused by partial alignment of the protein by a dilute liquid crystalline phase, but only under assumption that the CSA tensors are identical for all nitrogen atoms in the backbone.[10,11]

In principle the high-resolution NMR methods should open the possibility to measure $\Delta\sigma_{eff}$ and f_{orient} for each site along the protein chain and obtain information about the site-to-site variations.

More detailed knowledge of these parameters would enable more precise determination of local protein dynamics by NMR relaxation methods. The site-to-site variability of the CSA parameters has been assessed in a few studies of NMR relaxation on uniformly ^{15}N labeled proteins, in particular ubiquitin and ribonuclease H. The results are still somewhat ambiguous. The first report on site-specific values of CSA of amide ^{15}N in ubiquitin showed variations in a range from -116 to -231 ppm,[3,5] and the corresponding range for ribonuclease H was -129 to -213 ppm. The site-to-site variability was however not quite statistically significant, since the experimental errors were large.

The present study was undertaken with certain new theoretical and experimental approaches to assess the site-to-site variability of the amide ^{15}N CSA parameters in ubiquitin with 76 amino acid residues. NMR relaxation has been studied at four different magnetic fields, corresponding to 400, 500, 600, and 800 MHz proton resonance frequency. To minimize the relaxation contribution from other protons than the amide protons, the protein had all its nonexchangeable protons as ^{2}H and the amide protons back exchanged to ^{1}H. Our results were combined with those of two previous studies on ubiquitin.[4,5] From the field dependence of the relaxation parameters, the CSA parameters $\Delta\sigma_{eff}$ and f_{orient} and their experimental uncertainties were estimated for 70 of the 76 residues in ubiquitin (i.e., only N-terminus, the three proline residues, and the two severely exchange broadened signals from residues E24 and G53 were left out). Statistical analysis of the combined results showed a limited but statistically significant site-to-site variability, both for the magnitude and for the orientation. Furthermore the site-to-site variability in the geometry dependent CSA, important for estimating dynamics from cross-correlation rates, and the variability of the CSA parameter important for detecting conformational exchange contributions to the decay of transverse magnetization from cross-correlation rates are assessed. The estimation of the variability of the latter CSA parameter leads to a certain improvement in the methodology.

Materials and Methods

Sample Conditions: Perdeuterated and uniformly ^{15}N-labeled ubiquitin was purchased from VLI Research Inc. in a sealed NMR tube under nitrogen atmosphere. The sample conditions were as follows: 1.5 mM ubiquitin, 50 μM DSS for chemical shift referencing, in 50 mM phosphate buffer at pH 5.8 in 90% H_2O and 10% D_2O. All experiments were performed at 298 K.

NMR: Varian INOVA spectrometers equipped with inverse detection probes with pulsed field gradient along the *z*-axis were used, operating at 400, 500, 600, and 800 MHz proton resonance frequencies.

The steady-state NOE, longitudinal relaxation rate R_1, and the transverse relaxation rate R_2 were measured using the sequences of Farrow et al.[12] R_2 was measured using a continuous spin-lock with a field strength of 1.5 kHz (i.e., $R_{1\rho}$). The cross-correlation rates were measured using two-dimensional counterparts of the pulse sequences used in Damberg et al.[9] For the transverse cross-correlation experiments, the relaxation delay part of the sequences was modified. In the beginning of the relaxation delay, a 90° pulse on the nitrogen channel transforms the longitudinal magnetization into transverse. In the middle of the relaxation delay, a 180° pulse on the nitrogen channel was used for refocusing the chemical shift evolution. The last 90° pulse in the relaxation delay, which transforms the longitudinal magnetization mode to transverse magnetization suitable for PEP (preservation of equivalent pathways) transfer[13] with gradients[14] to proton magnetization for detection, was omitted in the transverse cross-correlation experiments, since the magnetization is already transverse at that point in that particular experiment.

For the perdeuterated ubiquitin sample the amide protons relax rather slowly. Therefore relatively long recycling delays of 5 s were employed. For the steady-state NOE even longer delays were used, to avoid nonequilibrium nitrogen magnetization in the reference experiments without proton saturation. Recycling delays of 15 s were used at 18.78 T and 10 s at the lower fields.

Typically 64 complex points were acquired in the indirectly detected dimension, and 2048, in the proton dimension. 16 or 8 transients were coadded. Approximately 10 2D spectra were acquired for each auto relaxation rate.

Rate Extraction: The transverse auto relaxation rates, R_2, were determined by the two-parameter fitting of functions of the form $A_0 \exp(-Rt)$ to the maximum peak heights as functions of time (t). Each trace along the directly detected dimension was individually baseline corrected with a low order polynomial.

The transverse relaxation rates, R_2, were subsequently corrected for off-resonance effects.[15]

The transverse cross-correlation rates were determined from both the buildup of in-phase magnetization from antiphase magnetization and the decay of antiphase magnetization, and the other way around, i.e., the buildup of antiphase magnetization from in-phase magnetization and the decay of in-phase magnetization, similar to ref 16. By dividing the product of the two buildup curves at any time point by the product of the two decay curves at the same time point, a data set is obtained which is independent of the efficiency by which antiphase and in-phase magnetizations modes are created and transferred to detectable proton in-phase magnetization. A function of the form $\tanh^2(\eta_{xy}t)$ was then fitted to the data. The data were given different weights to account for the higher uncertainty in the ratio for long relaxation times. These weighting factors were obtained by error propagation in a simulation where two coupled differential equations were used to describe the coupled relaxation, with typical values for the rates as input.

The decay rates of longitudinal two-spin order, the decay rates of longitudinal magnetization, R_1, and the longitudinal cross-correlation rates, η_z, were determined as in Damberg et al.[9] with an eight-parameter

(10) Boyd, J.; Redfield, C. *J. Am. Chem. Soc.* **1999**, *121*, 7441−2.
(11) Cornilescu, G.; Bax, A. *J. Am. Chem. Soc.* **2000**, *122*, 10143−54.
(12) Farrow, N. A.; Muhandiram, R.; Singer, A. U.; Pascal, S. M.; Kay, C. M.; Gish, G.; Shoelson, S. E.; Pawson, T.; Formankay, J. D.; Kay, L. E. *Biochemistry* **1994**, *33*, 5984−6003.
(13) Cavanagh, J.; Palmer, A. G.; Wright, P. E.; Rance, M. *J. Magn. Reson.* **1991**, *91*, 429−36.
(14) Kay, L. E.; Keifer, P.; Saarinen, T. *J. Am. Chem. Soc.* **1992**, *114*, 10663−5.
(15) Davis, D. G.; Perlman, M. E.; London, R. E. *J. Magn. Reson.* **1994**, *104*, 266−75.
(16) Pelupessy, P.; Espallargas, G. M.; Bodenhausen, G. *J. Magn. Reson.* **2003**, *161*, 258−64.

global fit to the data from the six experiments, the decay of two-spin order with and without cross-correlation suppression, the decay of longitudinal nitrogen magnetization (R_1) with and without cross-correlation suppression, the buildup of two-spin order from longitudinal nitrogen magnetization, and the buildup of nitrogen magnetization from longitudinal two-spin order.

The cross-relaxation rates, σ_{HN}, were calculated from the steady-state NOE and the R_1 rates.

Extracting CSA Magnitudes and Orientation Parameters. The principle for obtaining the CSA parameters from relaxation rates is to separate the dynamics and the interaction coefficients.[5,9] This goal is achieved by forming ratios between linear combinations of relaxation rates, proportional to the same linear combinations of spectral densities, as described below. The transverse and longitudinal CSA/dipole−dipole cross-correlation rates are proportional to $4J(0) + 3J(\omega_N)$ and $J(\omega_N)$,[17] respectively. For isotropic rotation the rates are given by

$$\eta_{xy} = -cdf_{orient}3^{1/2}/6\,(4J(0) + 3J(\omega_N)) \quad (1a)$$

$$\eta_z = -cdf_{orient}3^{1/2}J(\omega_N) \quad (1b)$$

Here η_{xy} and η_z are the transverse and longitudinal cross correlation rates, respectively. The coefficient $c = \gamma_N B_0 \Delta\sigma_{eff}\, 3^{-1/2}$, where the effective shielding anisotropy, $\Delta\sigma_{eff} = (\sigma_{xx}^2 + \sigma_{yy}^2 + \sigma_{zz}^2 - (\sigma_{xx}\sigma_{yy} + \sigma_{xx}\sigma_{zz} + \sigma_{yy}\sigma_{zz}))^{1/2}$, and σ_{xx}, σ_{yy}, and σ_{zz} are the principal values of the symmetric rank 2 shielding tensor. The coefficient $d = (\mu_0/4\pi)(h/2\pi)\gamma_H\gamma_N/r_{eff}^3$, where γ_N is the gyromagnetic ratio of the ^{15}N nuclear spin, B_0 is the magnetic field, μ_0 is the permeability of vacuum, h is Planck's constant, γ_H is the gyromagnetic ratio of the ^{1}H nuclear spin, and r_{eff} is the effective distance between the hydrogen and the nitrogen atomic nuclei; i.e., r_{eff} is a slightly longer distance than the equilibrium bond length accounting for the reduction of the strength of the dipolar coupling caused by vibrational motions. The factor f_{orient} is the orientation factor related to the orientation of the principal axes of the shielding tensor relative to the NH bond vector[9] defined as $f_{orient} = ((\sigma_{xx} - \sigma_{yy})(3\cos^2\theta_{x,r} - 1)/2 + (\sigma_{zz} - \sigma_{yy})(3\cos^2\theta_{z,r} - 1)/2)/\Delta\sigma_{eff}$, where $\theta_{x,r}$ and $\theta_{z,r}$ are the angles between the x and z principal axes and the NH bond, respectively. For the special case of an axially symmetric CSA tensor $\Delta\sigma_{eff} = |\sigma_{||} - \sigma_\perp|$, where $\sigma_{||}$ and $\sigma_\perp$ are the principal values of the shielding tensor associated with the symmetry axis and orthogonal to the symmetry axis, respectively. In the special case of an axially symmetric CSA tensor, $f_{orient} = 1.5\cos^2\beta - 0.5$ if $\sigma_{||} > \sigma_\perp$, and $f_{orient} = -(1.5\cos^2\beta - 0.5)$ if $\sigma_{||} < \sigma_\perp$, where β is the angle between the symmetry axis of the CSA tensor and the NH bond.

It is possible to obtain expressions, containing auto relaxation rates, proportional to the same linear combinations of spectral densities as in eq 1 from the spectral density mapping approach[18] in the absence of conformational exchange contributions to R_2 and under the assumption of isotropic rotation. Because of the difficulties associated with the measurement of proton relaxation rates, expressions were derived based on the reduced spectral density mapping formalism.[19−22] We obtain

$$R_2 - j_{trans}\sigma_{HN} = (3d^2 + 4c^2)/24(4J(0) + 3J(\omega_N)) \quad (2a)$$

$$R_1 - j_{long}\sigma_{HN} = (3d^2 + 4c^2)/4J(\omega_N) \quad (2b)$$

Here $j_{trans} = ({}^1/_2 J(\omega_H - \omega_N) + 3J(\omega_H) + 3J(\omega_H + \omega_N))/(-J(\omega_H - \omega_N) + 6J(\omega_H + \omega_N))$ and $j_{long} = (J(\omega_H - \omega_N) + 6J(\omega_H + \omega_N))/(-J(\omega_H - \omega_N) + 6J(\omega_H + \omega_N))$. The coefficients j_{trans} and j_{long} can be evaluated if an approximate spectral density function defined for the interval between $\omega_H - \omega_N$ and $\omega_H + \omega_N$ is available. In this study, the high-frequency part, i.e., between $\omega_H + \omega_N$ at 9.39 T ($\omega/2\pi = 360$ MHz) and $\omega_H - \omega_N$ at 18.78 T ($\omega/2\pi = 880$ MHz), of the spectral density function was approximated by a function of the form: $J(\omega) = a_1 + a_2/\omega^2$, with the boundary condition that $a_1, a_2 \geq 0$. The parameters a_1 and a_2 are fitted to the field dependent cross relaxation rates available at four different fields. The coefficients j_{trans} and j_{long} are calculated using the estimates of a_1 and a_2. It is noted that equivalents to j_{trans} and j_{long} have been derived previously under the assumption that the high-frequency part of $J(\omega) \propto 1/\omega^2$, resulting in $j_{trans} = 1.0785$ and $j_{long} = 1.249$.[23] In the approximation that the high-frequency part of the spectral density function is frequency independent $j_{trans} = {}^{13}/_{10}$ as reported in ref 5. Under the same approximation $j_{long} = {}^7/_5$ as reported in ref 19.

The ratio between eqs 2a and 1a and the ratio between eqs 2b and 1b are independent of the spectral densities. The ratios between the left-hand sides of the equations can therefore be used to define ratios that are independent of the dynamics:

$$q_{trans} \equiv (R_2 - j_{trans}\sigma_{HN})/\eta_{xy} \quad (3a)$$

$$q_{long} \equiv (R_1 - j_{long}\sigma_{HN})/\eta_z \quad (3b)$$

In the absence of conformational exchange contributions to the transverse autorelaxation, the ratios q_{trans} and q_{long} are equal and termed q in the following. The ratio q depends only on the magnitude and orientation of the CSA as

$$q = -(3d^2 + 4c^2)/(4\,3^{1/2}cdf_{orient}) \quad (4)$$

The effect from rotational anisotropy on the experimental q-values can be accounted for in an approximate way by calculating the theoretical relaxation rates for the NH spin pairs in a rigid structure from the rotational diffusion tensor using an assumed CSA with an assumed orientation. The correction factors are obtained by evaluating the q-value for the assumed interaction coefficients using eq 4 and dividing by the q-values obtained from the theoretical relaxation rates using eqs 3a and b.

When the product of B_0 and q is plotted as a function of the square of B_0, the data should fall on a straight line with slope k and intercept m.

$$B_0 q = kB_0^2 + m \quad (5)$$

From the slope and the intercept it is possible to estimate both the effective magnitude and the orientation factor of the CSA tensor.

$$\Delta\sigma_{eff} = \frac{3}{2}\frac{\mu_0}{4\pi}\frac{h}{2\pi}\frac{\gamma_H}{r_{eff}^3}\sqrt{\frac{k}{m}} \quad (6a)$$

$$f_{orient} = \pm\frac{1}{2\sqrt{km}} \quad (6b)$$

The sign of f_{orient} can be traced from the sign of the cross-correlation rate.[9] For the amide nitrogen atoms in ubiquitin studied here, the orientation factors are all negative.

The product of the orientation factor and the effective CSA has been estimated in several studies[4,24] and has been referred to as geometry-dependent CSA, CSA_g.[4] The CSA_g can be evaluated from the intercept, m, as

$$CSA_g = \Delta\sigma_{eff}\, f_{orient} = -\frac{\mu_0}{4\pi}\frac{h}{2\pi}\frac{3}{4}\frac{\gamma_H}{r_{eff}^3}\frac{1}{m} \quad (7)$$

The intercept is insensitive to conformational exchange contributions

(17) Goldman, M. *J. Magn. Reson.* **1984**, *60*, 437−52.
(18) Peng, J. W.; Wagner, G. *Biochemistry* **1992**, *31*, 8571−86.
(19) Lefevre, J. F.; Dayie, K. T.; Peng, J. W.; Wagner, G. *Biochemistry* **1996**, *35*, 2674−86.
(20) Peng, J. W.; Wagner, G. *Biochemistry* **1995**, *34*, 16733−52.
(21) Farrow, N. A.; Zhang, O. W.; Szabo, A.; Torchia, D. A.; Kay, L. E. *J. Biomol. NMR* **1995**, *6*, 153−62.
(22) Ishima, R.; Nagayama, K. *J. Magn. Reson.* **1995**, *108*, 73−6.
(23) Kroenke, C. D.; Loria, J. P.; Lee, L. K.; Rance, M.; Palmer, A. G. *J. Am. Chem. Soc.* **1998**, *120*, 7905−15.

to the decay of transverse magnetization. Therefore it is possible to estimate CSA_g from the transverse relaxation rates also for sites experiencing exchange. This statement is valid as long as the exchange contribution is proportional to the square of the magnetic field, i.e., when the exchange is very fast compared to the difference in resonance frequencies between the interconverting states. Furthermore, the effective strength of the off-resonance spin-lock field[25] or the pulse repetition rate has to be much lower than the exchange time constant or kept the same at all static field strengths used, and temperature variations between the experiments must be negligible so that the exchange contributions do not deviate from being proportional to the square of the magnetic field.

The q-values are interesting in themselves, since they are directly useful when estimating the exchange-free R_2 rate from the transverse cross-correlation rate, for example as

$$R_2^{\text{exchange-free}} = q\eta_{xy} + j_{\text{trans}}\sigma_{\text{HN}} \quad (8)$$

Equation 8 is similar to the equation presented in ref 26 but includes here a term with σ_{HN}, which accounts for the (generally small) contribution to transverse relaxation from high-frequency components of the spectral density function. When the expression for q_{long} (equation 3b) is inserted into eq 8, with j_{long} and j_{trans} derived from the $1/\omega^2$ approximation, one obtains an expression that is equivalent to the expression given in ref 23.

From the linear fitting procedure it is clear that the value of B_0q is most precisely interpolated in the center of the available data, i.e., at the average squared field strength. The value of q at this particular magnetic field, where site-to-site variations in q are easiest to detect, can be calculated as

$$q(B_0^{\text{opt}}) \equiv \langle B_0 q\rangle / \sqrt{\langle B_0^2\rangle} \quad (9)$$

Here the angular brackets indicate averaging over the available data for one studied nucleus. The value of q at the magnetic field B_0^{opt} can also be calculated from the estimates of $\Delta\sigma_{\text{eff}}$ and f_{orient} using eq 4 or from the k and m values as $q = (B_0^2k + m)/B_0$.

Results

In Figure 1 the typical buildup and decay of longitudinal magnetization, used for determining the longitudinal cross-correlation rate, are shown for ^{15}N of I13 of ubiquitin, together with the fitted curves according to ref 9. The measured rates for all residues in ubiquitin can be found in the Supporting Information together with crude estimates of the uncertainties based on linear approximations in the nonlinear fits. The experimental rates were used to evaluate q-values according to eqs 3a and b. The j_{trans} and j_{long} coefficients were obtained by approximating the spectral density function in the interval between $\omega/(2\pi) = 360$ MHz and $\omega/(2\pi) = 880$ MHz as $J(\omega) = a_1 + a_2/\omega^2$. The coefficients a_1 and a_2 were determined by fitting them to the field dependence of the cross-relaxation rates, which depend solely on spectral densities in this interval. The obtained j-coefficients are numerically similar to the coefficients presented in ref 23 derived using the assumption that the high-frequency part of the spectral density function is proportional to $1/\omega^2$, in accordance with decreasing cross-relaxation rates with increasing field.

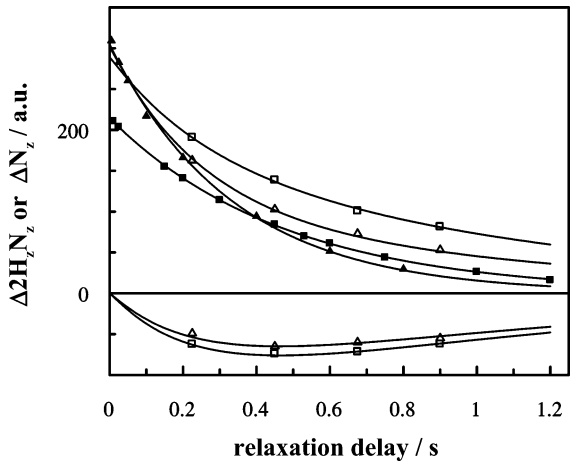

Figure 1. Typical example of the time-evolution of longitudinal ^{15}N magnetization (squares) and longitudinal two-spin order (triangles) for the amide nitrogen-proton spin pair in the amino acid residue I13 in ubiquitin. Solid symbols represent data acquired when cross-correlation effects were suppressed, while open symbols represent data when cross-correlation was active. On the positive side of the vertical axis, the decays are monitored, while the buildups from the other magnetization mode give the negative signals. The curves show the corresponding fitted model (cf. ref 9), with eight adjustable parameters (R_1, η_z, the auto relaxation rate of longitudinal two-spin order, initial amplitudes of the two-spin order, and longitudinal nitrogen magnetization in the experiments where cross-correlation is active, the relative efficiency by which longitudinal two-spin order and nitrogen magnetization are converted to detectable in-phase proton magnetization, and two amplitudes in the auto relaxation experiments where cross-correlation effects are suppressed).

Rotational anisotropy may make the spectral density functions for the CSA and dipolar interactions unequal. This effect has been exploited previously to estimate the magnitude and orientation of the assumed axially symmetric backbone ^{15}N CSA tensor in lysozyme.[7] In the present study the q-values were corrected for the effect of rotational anisotropy as described above. The correction factors were calculated using the ubiquitin structure refined against residual dipolar couplings.[11] An axially symmetric rotational diffusion tensor was used with a rotational anisotropy of 1.17, and angles describing the orientation of the symmetry axis of the rotational diffusion tensor relative to the pdb coordinates θ and φ were set to 40° and 46°, respectively, as previously determined.[27] The theoretical relaxation rates were calculated using a CSA tensor with $\sigma_{zz} = -108.5$ ppm in the peptide plane close to orthogonal to the peptide bond making an angle $\theta_{z,r} = 19°$ with the NH bond, $\sigma_{yy} = 45.7$ ppm orthogonal to the peptide plane ($\theta_{y,r} = 90°$), and $\sigma_{xx} = 62.8$ ppm orthogonal to the other two as obtained by Cornilescu and Bax in their alignment study.[11] The correction for rotational asymmetry changed the q-values by less than 1%.

Incorporation of Published Data. The q_{trans} and q_{long} values were also evaluated at 11.74 T from the experimental rates determined by Kövér and Batta[4] and corrected for rotational asymmetry. From the η/R_2 ratios reported by Fushman et al.,[5] q_{trans} values were estimated at 8.45, 11.74, and 14.09 T. To account for the small contribution from heteronuclear cross-relaxation, the inverse of the η/R_2 ratios were rescaled by factors $((R_2 - j_{\text{trans}}\sigma_{\text{HN}})/R_2)$ calculated from the relaxation rates reported by Lee and Wand[28] to obtain the q_{trans}. For the 8.45 T data the

(24) Tjandra, N.; Szabo, A.; Bax, A. *J. Am. Chem. Soc.* **1996**, *118*, 6986−91. What the authors call CSA^{red}/S^2 is an estimate of CSA_g.
(25) Akke, M.; Palmer, A. G. *J. Am. Chem. Soc.* **1996**, *118*, 911−2.
(26) Zeeb, M.; Jacob, M. H.; Schindler, T.; Balbach, J. *J. Biomol. NMR* **2003**, *27*, 221−34.
(27) Tjandra, N.; Feller, S. E.; Pastor, R. W.; Bax, A. *J. Am. Chem. Soc.* **1995**, *117*, 12562−6.
(28) Lee, A. L.; Wand, A. J. *J. Biomol. NMR* **1999**, *13*, 101−12.

correction factors were derived from the R_2 and cross-relaxation rates reported here for 9.39 T. This approach reduces the q-values by approximately 2% for all sites, with only small site-to-site variations. Thereafter they were corrected for the small effect of rotational anisotropy.

To improve the comparison between q-values obtained from different experiments, a rescaling procedure was used. The 12 averages of B_0q_{trans} or B_0q_{long} over the sites from each field and each dataset were calculated. The sites that are affected by conformational exchange broadening (D23 and N25) and the data with increased uncertainty due to hydrogen exchange with water (L8, T9, G10, N25, A46, D58, S65, R74, G75), slow relaxation (R74, G75, G76), or where data is missing in any of the data sets derived from refs 4 and 5.

Consistency Testing. The uncertainties in the rates were propagated to the q-values using the error propagation formula. Uncertainties derived this way can be underestimated, since they mainly include uncertainties due to spectrometer noise and not errors due to model inconsistencies, like anisotropic motions, violations of the basic assumptions in reduced spectral density mapping or conformational exchange contributions to R_2, etc. The errors might also be underestimated due to certain off-resonance effects,[29] less than optimal pulse sequences,[16] or other experimental shortcomings. To include also such error sources, the uncertainty estimates were rescaled according to a simple consistency test based on comparing the sample variances of q_{long} and q_{trans} at a particular field. The details of the test are described in the Supporting Information. The uncertainties were generally increased by up to a factor of 3.

Site-Specific Linear Fitting. The corrected B_0q values were used in 70 weighted linear fits according to eq 5. For the sites that are known to have contributions to the apparent R_2 from conformational exchange (D23 and N25) only the B_0q_{long} values were used. The inverse of the square of the rescaled uncertainties were used as weighting factors. In Figure 2 the results are exemplified by the data from I13.

The intercepts, m, and the corresponding slopes, k, are semiconfounded. The joint confidence regions for k and m are given by weighted sum of squares (SoS) contours in the SoS vs k and m graph. An iso SoS curve with the SoS $= S_R[1 + p/(n - p)F_\alpha(p,n - p)]$ enclose the $1 - \alpha$ joint confidence region. S_R is the minimum weighted sum of squares for the best fitting line, p is the number of parameters, n is the number of observations, and $F_\alpha(p,n - p)$ is the upper 100 α % point of the F distribution with p and $n - p$ degrees of freedom.[30] Such iso SoS curves are error ellipsoids representing the joint uncertainty of k and m. The contour levels are transformed to the $\Delta\sigma_{eff}$ and f_{orient} space. In Figure 3 joint confidence regions for the amide nitrogen atoms in the I13 and I36 residues are shown as typical examples. From this figure it is apparent that despite the difficulties to separate the $\Delta\sigma_{eff}$ and f_{orient}, it is clear that the CSA tensors are not equal for the two nitrogen atoms, since the confidence regions do not overlap.

Table 5S shows the CSA parameters ($\Delta\sigma_{eff}$ and f_{orient}) evaluated here for all 70 amide nitrogen atoms showing a cross-peak in the HSQC spectrum of ubiquitin, the associated uncertainties, and the asymptotic correlation coefficients between $\Delta\sigma_{eff}$ and f_{orient}.

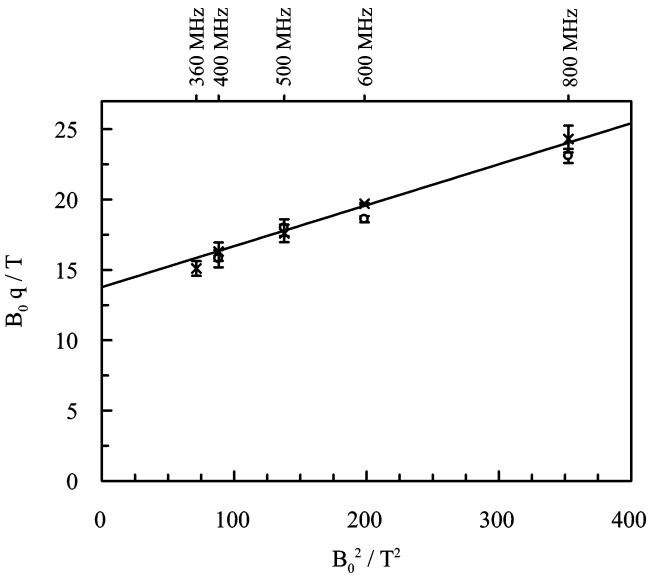

Figure 2. Graph illustrates the linear fit to the data measured here and from refs 4 and 5 for the nitrogen atom in I13 of ubiquitin. The crosses represent B_0q_{trans} and the open circles represent B_0q_{long}. For the 500 MHz data weighted averages of the two B_0q_{long} values and the three B_0q_{trans} values are shown. Error bars indicate 68% confidence intervals.

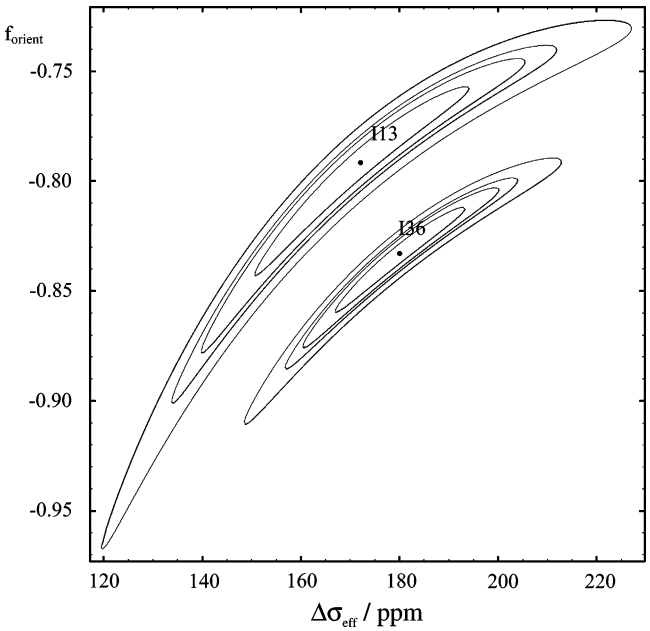

Figure 3. Joint confidence regions for $\Delta\sigma_{eff}$ and f_{orient} for the nitrogen atoms in residues I13 and I36 in ubiquitin. The contour levels enclose 68%, 90%, 95%, and 99% confidence regions and were derived as described in the text.

Statistical Analysis of the Results. A. CSA Magnitudes: The site-specific $\Delta\sigma_{eff}$ values are obtained from the slopes k and the intercepts m using eq 6a, assuming $r_{eff} = 1.041$ Å as found from the analysis of residual dipolar couplings[31] and subsequently reproduced in quantum chemical calculations.[32] The $\Delta\sigma_{eff}$ values are displayed as a function of the ubiquitin sequence in Figure 4. The associated uncertainties are calculated

(29) Korzhnev, D. M.; Tischenko, E. V.; Arseniev, A. S. *J. Biomol. NMR* **2000**, *17*, 231−7.
(30) Box, G.; Hunter, W.; Hunter, S. Statistics for experimenters. New York: John Wiley & Sons: 1978.
(31) Ottiger, M.; Bax, A. *J. Am. Chem. Soc.* **1998**, *120*, 12334−41.
(32) Case, D. A. *J. Biomol. NMR* **1999**, *15*, 95−102.

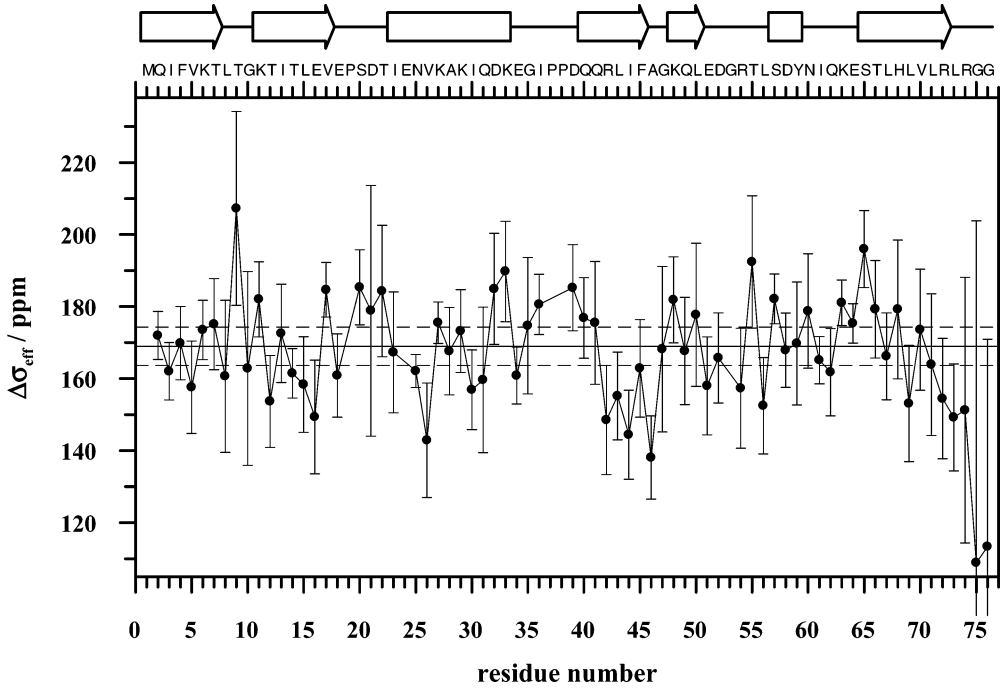

Figure 4. $\Delta\sigma_{eff}$ estimates as a function of the ubiquitin sequence from the present measurement combined with the data presented in refs 4 and 5. The error margins show 68% (one standard deviation) confidence intervals and were estimated from the weighted sum of squares in the linear fit (the confidence intervals for G75 and G76 extend below the graph). The horizontal solid line indicates the maximum likelihood estimate of the population mean, and the dashed horizontal lines indicate + and − one standard deviation of the true distribution. The secondary structure elements and the amino acid sequence are indicated above the graph.

from the uncertainties in the slopes and intercepts, and their covariances, using the error propagation formula.

The CSA values distribute between 192 ± 10 ppm for T55 and 143 ± 16 ppm for V26, when we exclude the data from the very flexible C-terminal residues and the sites where the amide proton is exchanging with water with a rate comparable to the relaxation rates, and consequently are associated with higher uncertainty. Under the assumptions that the true CSA values are normally distributed with mean μ and variance Λ^2 and that the uncertainty estimates are correct, maximum likelihood estimates of the population mean and the true site-to-site variability can be obtained. The likelihood function is written as

$$p = \prod_{i=1}^{70} \frac{1}{\sqrt{2\pi(\Lambda^2 + s_i^2)}} \exp\left(-\frac{(\mu - x_i)^2}{2(\Lambda^2 + s_i^2)}\right) \qquad (10)$$

where x_i and s_i are the experimentally determined values and associated uncertainties for the nuclei $i = 1....70$. The likelihood function is maximized for $\mu_{CSA} = 169$ ppm and $\Lambda_{CSA} = 5.3$ ppm. A 95% confidence interval, estimated from the second derivative of the natural logarithm of the likelihood function, spans from 166 to 172 ppm for μ and from 1.4 to 9.4 ppm for Λ.

B. Orientation Parameters: The site-specific orientation parameters are calculated from m and k using eq 6b and are shown in Figure 5. They fall within the range −0.93 for V26 and −0.71 for G47, when the data with increased uncertainty are excluded. The population mean and site-to-site variability are estimated by maximizing the likelihood function (equation 10). The population mean is −0.80 with a 95% confidence interval spanning from −0.81 to −0.79. The site-to-site variability is estimated to 0.04 with a 95% confidence interval spanning from 0.03 to 0.05. The uncertainties in the site-specific estimates are in many cases smaller than the site-to-site variations.

C. Geometry Dependent CSA: The product of $\Delta\sigma_{eff}$ and f_{orient} is denoted CSA_g. It is the interaction strength for the CSA/dipole−dipole cross-correlation. The site-specific CSA_g values are shown in Figure 6. They are calculated from the intercepts using eq 7 and fall within the range −119 ppm for G47 and −158 for K11, when the data with increased uncertainty are excluded.

The maximum likelihood estimate of the population mean is −135.5 ppm with a 95% confidence interval spanning from −137 to −133 ppm. The site-to-site variability is estimated to 5 ppm with a 95% confidence interval spanning from 3.2 to 6.7 ppm.

D. $q(B_0^{opt})$ Parameter: The q-values at a particular field within the range of used fields are less challenging to derive from the experimental relaxation rates than the CSA parameters studied above, since such q-values are obtained by interpolation rather than extrapolation. We chose to evaluate the values of q at a magnetic field of 13.0 T corresponding to 552 MHz proton resonance frequency, for optimal comparison to the ribonuclease H values evaluated from published relaxation rates (vide infra). The q-values, which are corrected for rotational anisotropy and systematic bias as described above, are independent of the dynamics and only sensitive to the shielding anisotropy, although in a somewhat intricate way (eq 4).

The derived values are displayed in Figure 7. They fall in the range between 1.28 for K11 and 1.62 for G47. The maximum likelihood estimate of the average is 1.43 with a 95% confidence interval spanning from 1.41 to 1.44. The variability is estimated to 0.063 with a 95% confidence interval spanning

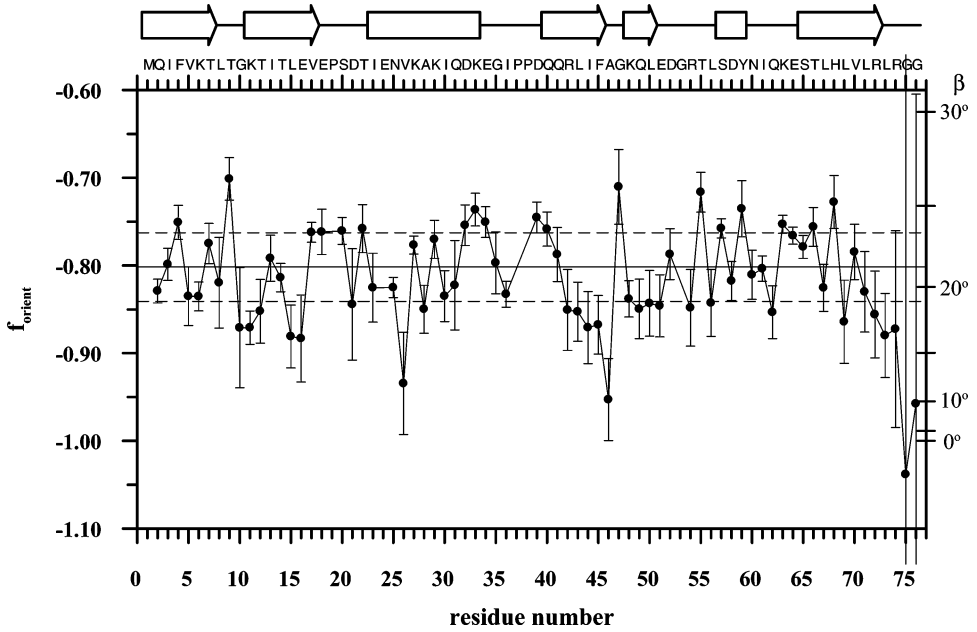

Figure 5. Graph illustrates the site-specific estimates of f_{orient} from the present measurements combined with the data presented in refs 4 and 5. The error bars correspond to one standard deviation. The solid horizontal line indicates the maximum-likelihood estimate of the average. The dashed lines indicate + and − one standard deviation of the true distribution as obtained from the maximum likelihood calculation. In the approximation of an axially symmetric CSA tensor, the orientation factor corresponds to an angle, β, between the symmetry axes of the CSA and dipolar interactions. Such angles can be obtained from the scale to the right.

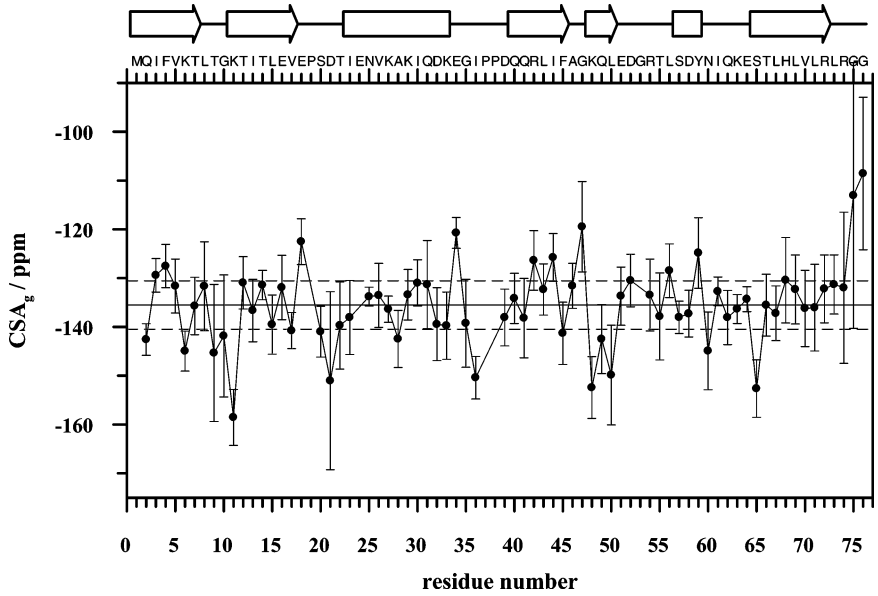

Figure 6. Graph illustrates the site-specific estimates of the CSA_g parameters from the present measurements combined with the data reported in refs 4 and 5. The error bars correspond to one standard deviation. The solid horizontal line indicates the maximum-likelihood estimate of the average. The dashed lines indicate + and − one standard deviation of the true distribution as obtained from the maximum likelihood calculation.

from 0.053 to 0.076. Clearly the uncertainties in the site-specific estimates are significantly smaller than the variability. A variability of 0.063 around 1.43 corresponds to 4.4%. This percentage is a number highly relevant to approaches where the exchange-free R_2 rate is estimated from the transverse cross-correlation rate η_{xy} (eq 8).

Searching for Systematic Variation in $q(B_0^{opt})$. To expand the size of the relaxation database, the experimental rates reported in ref 3 for *Escherichia coli* ribonuclease H were reevaluated to find site-specific values for $q(B_0^{opt})$ according to eq 9 (from this dataset the simultaneous determination of both the orientation factor and the effective anisotropy could not be performed reliably due to a smaller variation in static magnetic field). Longitudinal and transverse cross-correlation rates as well as R_1, R_2 and the heteronuclear NOEs are available from both 11.7 and 14.1 T. Values of q were evaluated using eqs 3a and 3b. The $q(B_0^{opt})$ values were evaluated separately for longitudinal and transverse data, using eq 8, and correspond to q-values at 13.0 T. The resulting $q(B_0^{opt})$-values were analyzed by a two-factor ANOVA analysis,[30] treating the sites as 81 blocks and the two methods (equation 3a and 3b) as two treatments. The analysis yields an average of 1.42 and an uncertainty in the site-specific values of 0.05. There are statistically significant site-to-site variations (p-value for the hypothesis that there are

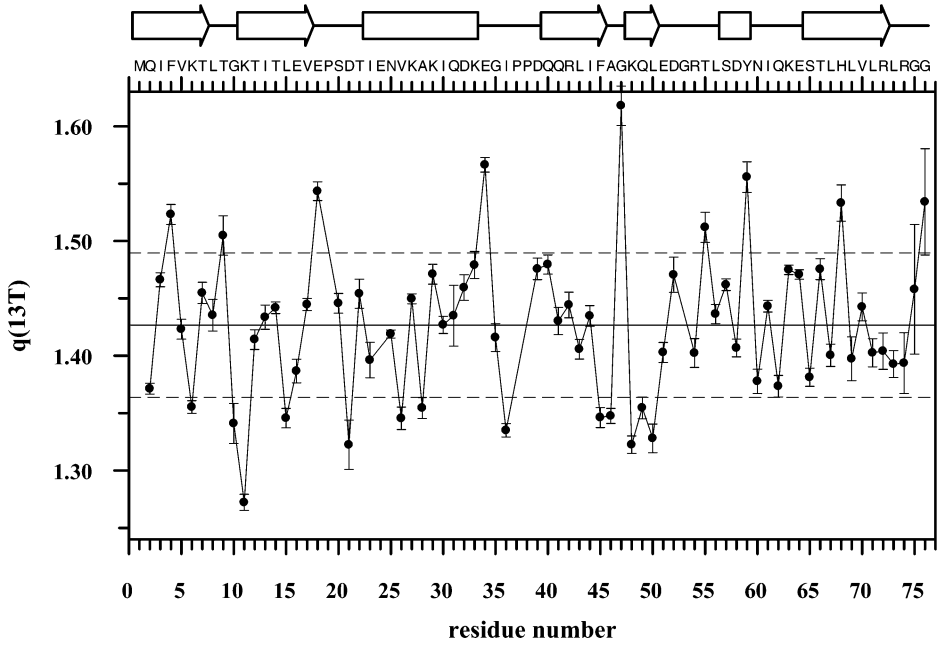

Figure 7. Site-specific estimates of q(13.0 T) derived from the linear fitting to the present measurements combined with the data presented in refs 4 and 5. The error bars correspond to one standard deviation. The solid horizontal line indicates the maximum-likelihood estimate of the average. The dashed lines indicate + and − one standard deviation of the true distribution as obtained from the maximum likelihood calculation.

no site-to-site variations is 1×10^{-4}, according to an F-test). The site-to-site variability has a point estimate of 0.06, in excellent agreement with the results for ubiquitin (0.063).

When combining the data from ubiquitin and ribonuclease H one obtains $70 + 81 = 151$ sites for which there are reliable values of q at 13.0 T. This dataset is large enough to be examined for differences between amino acid types, etc.

A. Correlation with Secondary Structure. When considering residues belonging to different types of secondary structure separately, no apparent difference between the averages of the q(13 T) values is found.

B. Correlation with Isotropic Nitrogen Shifts. Since all the CSA parameters as well as the isotropic chemical shift are functions of the principal components of the shielding tensor, there might exist correlations between them. In both the ubiquitin data and the ribonuclease H data, there is a tendency for atoms with low isotropic chemical shift to display high q(13 T) values (Figure 1S).

In the ubiquitin data there is a tendency for backbone nitrogen atoms with lower isotropic chemical shift to display larger $\Delta\sigma_{\mathrm{eff}}$ values (Figure 2S). Weighted linear regression yields $\Delta\sigma_{\mathrm{eff}} = 306.5 - 1.15\ \delta_{\mathrm{iso}}$. The statistical significance of the observed correlation was assessed by comparing the ratio between the observed slope −1.15 and the associated uncertainty 0.26 with a t distribution with 68 degrees of freedom. This test gives a p-value for the hypothesis that the true slope is zero of 3×10^{-5}, disproving the null hypothesis.

There is a tendency for backbone nitrogen atoms with higher isotropic chemical shifts to display lower (larger negative numbers) f_{orient} values, shown in Figure 8. Weighted linear regression yields $f_{\mathrm{orient}} = -0.15 - 0.005\ \delta_{\mathrm{iso}}$, when δ_{iso} is given in units of ppm. The p-value for the null hypothesis, that the slope is zero, is 2×10^{-12}.

When considering $\mathrm{CSA_g}$, which is the product of f_{orient} and $\Delta\sigma_{\mathrm{eff}}$, the correlations found above cancel each other so that no apparent correlation is observed (Figure 3S).

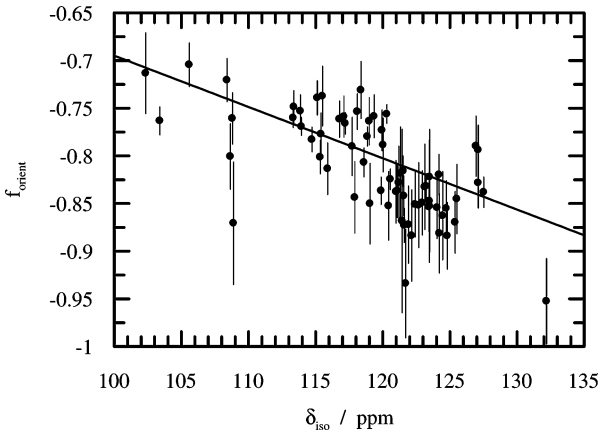

Figure 8. Graph illustrates the potential correlation between the observed f_{orient} values and the isotropic chemical shift in ubiquitin. The uncertain values from G75 and G76 are not included.

C. Correlation with Amino Acid Residue Type. The nitrogen atom in a glycine residue is adjacent to a methylene carbon, different from the nitrogen atoms in other residues, which have a methine carbon as the neighbor. Because of the different chemical environment one can expect different shielding properties. Lower isotropic chemical shifts for nitrogen atoms in glycine residues compared to the other residue types are indeed generally found. A two-tailed t-test was performed to look for differences in average q-values between the two groups, the 12 nitrogen atoms in glycine residues and the 139 backbone nitrogen atoms in other residue types. The q-values at 13.0 T for glycine residues distribute around an average of 1.51 with a standard deviation of 0.11, while the q-values for the other residue types distribute around an average of 1.41 with a standard deviation of 0.06. This corresponds to a significant difference (p-value for the hypothesis that there is no difference between the averages of the two groups is 0.014 according to a heteroscedastic two-tailed t-test). A table containing the

average q(13 T) values for each residue type can be found in the Supporting Information (Table 6S).

Discussion

A. CSA Magnitudes. There are several different conventions regarding how to denote shielding anisotropies. For the interpretation of relaxation data the convention used here is suitable. The $\Delta\sigma_{eff}$ value is the relaxation effective shielding anisotropy for an asymmetric CSA tensor. It is similar to, but not exactly the same as, the magnitude of the shielding anisotropy, $\Delta\sigma = (\sigma_{11} - (\sigma_{22} - \sigma_{33})/2)$, reported in alignment studies and solid-state NMR studies. The population mean of $\Delta\sigma_{eff}$ is estimated to 169 ppm. This value can be compared to values calculated from the results of the alignment studies. Using the data from the pioneering study on lysozyme by Boyd and Redfield,[10] our calculations result in slightly higher $\Delta\sigma_{eff}$, around 172 ppm, slightly dependent on which of their models one uses. Using the alignment data on ubiquitin by Cornilescu and Bax, we calculated $\Delta\sigma_{eff}$ to 163.4 ppm, using the numbers obtained from the refined NMR structure. The numbers are dependent on the NH bond length used in the analysis, in a similar way both for the alignment studies and for the linear fitting approach used here.

The site-to-site variability of the backbone ^{15}N shielding anisotropy along the polypeptide chain in ubiquitin is limited, with a point estimate of 5.3 ppm, with a 95% confidence interval spanning from 1.4 to 9.4 ppm. This finding is in contrast with earlier reports where the standard deviation of the observed anisotropies for ubiquitin, which is significantly larger, was used as a measure of the variability.[5]

One the other hand it is in excellent agreement with the results of Kroenke et al.[3] for ribonuclease H. In that study a point estimate of 5.5 ppm was obtained with an upper limit of their confidence interval at 9.5 ppm. The present result is also in agreement with the result of Cornilescu and Bax,[11] who estimated an upper limit of 17 ppm for the site-to-site variability in ubiquitin, from chemical shift changes upon weak alignment. It is also in accordance with the conclusions based on dynamic model fitting to multiple field relaxation data for the protein C2A-p8^{MTCP1}, where it was found that the CSA is almost invariant.[6]

Both the isotropic shift and the effective CSA are functions of the three principal values of the shielding tensor. If the three principal values varied independently with equal amplitude, one would expect the effective CSA to vary considerably more than the isotropic chemical shift. Furthermore, there would be no correlation between isotropic chemical shifts and $\Delta\sigma_{eff}$. We observe similar magnitudes of the variations in the isotropic chemical shifts and in the $\Delta\sigma_{eff}$ values and a tendency for atoms with low chemical shift to have high $\Delta\sigma_{eff}$ values, showing that the principal values of the shielding tensor change in a correlated manner. The approach that was used to estimate an upper limit for the variability from chemical shift changes of weakly aligned ubiquitin taken by Cornilescu and Bax[11] assumes that the principal values varied independently with equal amplitude. This is here shown to be an incorrect assumption.

CSA Parameters and NH Bond Distance. The evaluation of $\Delta\sigma_{eff}$ and CSA_g from the slope and the intercept in the linear fit depend on the NH bond distance (cf. eqs 6a and 7). Site-to-site variations in the NH bond length could consequently influence the observed site-to-site variations in $\Delta\sigma_{eff}$ and CSA_g. On the other hand f_{orient} and q(13 T) are evaluated from the relaxation rates without the need to consider the NH bond length (cf. eqs 6b and 9). Structural data at a sufficient resolution to resolve differences between the NH bond lengths at different sites are scarce. Quantum chemical calculations on model compounds indicate that the nature of the hydrogen bond may have a small effect. At the Hartree−Fock level Guo and Karplus[33] found that the NH bond length increased by 0.001 to 0.009 Å upon hydrogen bond formation. An educated guess could be that there are small site-to-site variations in the NH bond distance, on the order of 0.005 Å, consistent with a fractional site-to-site variability in $1/r_{eff}^3$ of ca. 1.5%. This rough estimate can be compared to the fractional site-to-site variabilities in $\Delta\sigma_{eff}$ ($^5/_{169} = 3\%$) and CSA_g ($^5/_{135} = 4\%$) observed here. A direct comparison of the percentages reveals that the variations in shielding anisotropy and NH bond distance may have approximately equal impact on the observed variability in $\Delta\sigma_{eff}$ and CSA_g. If the shielding tensors would have been independent of the NH bond distances, it might have been possible to partition the observed variations into a fraction caused by variations in the NH bond length and true CSA variations. It is well-known from quantum chemical calculations that the shielding tensors are exquisitely sensitive to the coordinates of the nuclei. Therefore partitioning of the observed variations is very difficult or even impossible at this stage. Preliminary quantum chemical calculations on a capped glygly dipeptide in the local minima with dihedral angles close to a β-strand indicate that as the NH bond is elongated, $\Delta\sigma_{eff}$ decreases slightly. In the present experimental study, where the product of $\Delta\sigma_{eff}$ and r_{eff}^3 can be determined directly from the slope and the intercept (cf. eq 6a), the two effects, i.e., $\Delta\sigma_{eff}(r_{NH})$ decreasing with increasing r_{NH} and $r_{eff}^3(r_{NH})$ increasing with increasing r_{NH}, partly cancel each other out in the product. Consequently we cannot determine whether site-to-site variations in the NH bond lengths lead to a small over, or under, estimation of the true variations in the anisotropic shielding. Until structural data with sufficient resolution to resolve the variations in NH bond distance along the sequence becomes available, we assume that the NH bond length is invariant and attribute the observed variations to variations in the shielding anisotropy.

How Does the Variability of $\Delta\sigma_{eff}$ Affect the Model-Free Paramters? To assess the potential bias of the dynamic parameters, i.e., the model-free parameters,[34] caused by using an assumed CSA when analyzing the relaxation rates obtained for a site with a different true CSA, numerical simulations were carried out. Synthetic data were generated from a dynamic model ($\tau_m = 4.0$ ns, $S^2 = 0.9$, and $\tau_e = 50$ ps) for magnetic fields of 9.39 and 18.78 T (corresponding to 400 and 800 MHz proton frequencies) for different values of $\Delta\sigma_{eff}$ between 143 and 183 ppm. The data were evaluated assuming $\Delta\sigma_{eff}$ to be 163 ppm, and the corresponding fitted values of the generalized squared order parameters, S^2, are shown in Figure 9. The error in the assumed $\Delta\sigma_{eff}$ value leaves the global correlation time estimates essentially unchanged while there is an obvious influence on S^2 (Figure 9).

The error in S^2 is proportional to the square of the magnetic field and proportional to the error in the shielding anisotropy.

(33) Guo, H.; Karplus, M. *J. Phys. Chem.* **1992**, *96*, 7273−87.
(34) Lipari, G.; Szabo, A. *J. Am. Chem. Soc.* **1982**, *104*, 4546−59.

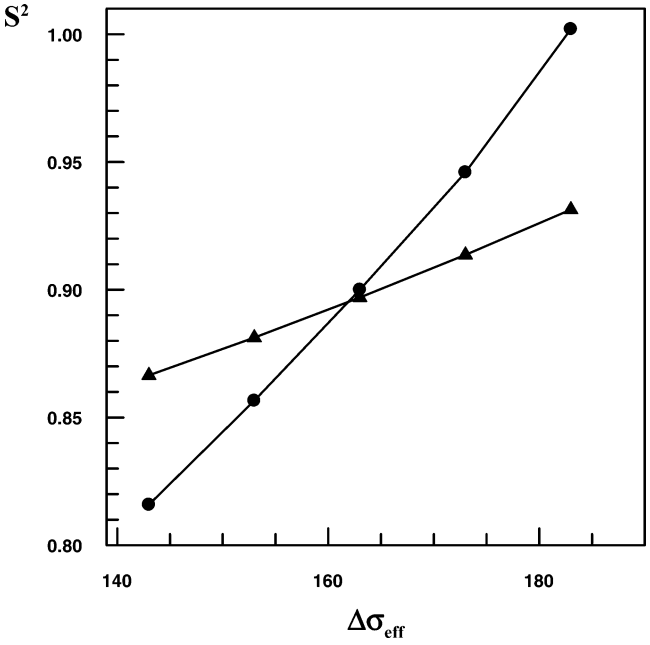

Figure 9. Apparent generalized squared order parameter, S^2, for a site with the true parameters $t_m = 4.0$ ns, $S^2 = 0.9$, and $t_e = 50$ ps as obtained when fitting the model-free parameters assuming $\Delta\sigma_{eff}$ of 163 ppm to data for a site with a true $\Delta\sigma_{eff}$ according to the horizontal axis. Solid circles represent 800 MHz and triangles 400 MHz.

If relaxation data are analyzed for a site with $\Delta\sigma_{eff}$ equal to 173 ppm and analyzed assuming $\Delta\sigma_{eff}$ equal to 163 ppm, the generalized order parameter will be overestimated by 5% at a magnetic field corresponding to a 800 MHz proton resonance frequency. A site-to-site variability of 5 ppm would consequently add approximately 3% uncertainty to the evaluated squared generalized order parameter for data obtained at a 800 MHz proton resonance frequency.

B. Orientation Factors. The orientation factors show a population mean of −0.80, which can be compared to the alignment studies[10,11] where the results translate to −0.84 and −0.83 for lysozyme and ubiquitin, respectively.

The variability is estimated to 0.04, with a 95% confidence interval spanning from 0.03 to 0.05. This corresponds to variations in the angle between the symmetry axis of an assumed axially symmetric CSA tensor and the NH bond of 2.3° around an average of 21.4° (calculated as $f_{orient} = -(3\cos^2\beta - 1)/2$.

Cornilescu and Bax[11] obtained a difference between residues in β-strands and in helices, in their alignment study, that translate into differences mainly in the orientation factors with −0.88 or −0.90 for helical residues, depending on whether the NMR or X-ray structure is used in the analysis, while an orientation factor of −0.82 or −0.80 is obtained for residues belonging to β-strands. This difference between different secondary structures is not supported by the current relaxation data. In the current analysis the uncertainty in the site-specific orientation factors is about 0.03. Therefore such a large variation is not likely to be hidden in white noise.

C. Geometry Dependent CSA. The CSA_g values distribute with an estimated average of −135.5 pm and an estimated variability of 5 ppm. From the alignment study of lysozyme[10] one can calculate a CSA_g value of −144 ppm. The value calculated from the alignment study on ubiquitin[11] is −135.5 ppm, which resembles the result obtained here more closely.

When the CSA_g value is known, it is straightforward to use measured cross-correlation rates to derive information about the flexibility and dynamics of a polypeptide. A variability of 5 ppm around −135.5 corresponds to approximately 4% in the CSA_g values. For the general situation when the site-specific CSA_g value is not known, the variability will propagate to an uncertainty in the squared generalized order parameter of approximately the same magnitude, i.e., around 4%.

D. *q*(13.0 T). The q(13.0 T) values for ubiquitin are distributed with an average of 1.43 and a site-to-site variability of 0.06. This variability matches the site-to-site variability of 0.06 obtained from the ANOVA analysis for the ribonuclease H data very well. In principle the q_{long} and q_{trans} data used in the ANOVA analysis for ribonuclease H are not quite independent because of their dependence on the cross-relaxation rate, σ_{HN}. The contributions from the cross-relaxation rates are at least 1 order of magnitude too small to have a serious effect on the ANOVA analysis.

Glycine Is Different. When analyzing the q(13.0 T) parameters, which are determined with a low fractional uncertainty, it is clear that glycine residues have a shielding anisotropy different from that of the other residue types. This is not very surprising considering that glycine residues show lower isotropic chemical shifts for the amide nitrogen than other residue types, and the same factors are likely to influence both isotropic and anisotropic chemical shifts. When comparing the solid-state NMR data reported for glycine residues[35] to solid-state NMR data for leucine and valine residues in various peptides,[36] it seems as if the three principal components of the anisotropic part of the shielding tensor are similar for the three residue types, while the angle between the NH bond vector and the closest component tends to be larger for nitrogen atoms in glycine residues than nitrogen atoms in valine and leucine residues. This is in agreement with the observation that the q(13 T) values are higher in glycine residues than in valine and leucine residues (cf. eq 4 where f_{orient} is in the denominator). An alternative explanation would be that $\Delta\sigma_{eff}$ tends to be higher in glycine residues, which is supported by a close examination of the data reported for ribonuclease H [3] which reveal larger magnitudes of the $\Delta\sigma$ values for nitrogen atoms in glycine residues compared to other residue types.

***q*-Values and Conformational Exchange.** The variability in q (around 4%) may dominate the uncertainty in the exchange-free R_2 rates, evaluated according to eq 8, since the transverse cross-correlation rate, η_{xy}, can be measured with high precision; uncertainty estimates below 2% are quoted in the literature.[24,37] Considering that the value of q(13.0 T) has a variability of approximately 4%, it is difficult to estimate q_{long} from experimental relaxation rates with a much higher precision. It might be better to use the average value estimated from the standard CSA parameters and propagate the uncertainty due to site-specific variations to the exchange term when using eq 8. If the rates for evaluating the q_{long} are available, the site-specific q_{long} is obtained with a significant uncertainty, comparable in magnitude to the variability of q. In such cases it is beneficial

(35) Lee, D. K.; Wittebort, R. J.; Ramamoorthy, A. *J. Am. Chem. Soc.* **1998**, *120*, 8868−74.
(36) Lee, D. K.; Wei, Y. F.; Ramamoorthy, A. *J. Phys. Chem. B* **2001**, *105*, 4752−62.
(37) Pang, Y.; Buck, M.; Zuiderweg, E. R. P. *Biochemistry* **2002**, *41*, 2655−66.

to use a weighted average of the site-specific value, q_{long}, and a value calculated from the standard CSA parameters, i.e., $\Delta\sigma_{eff} = 169$ ppm and $f_{orient} = -0.80$, when evaluating the exchange-free R_2 using eq 9, i.e., $q = wq_{long} + (1 - w)q_{standard}$, where w is the weighting factor. The weighting factors should be chosen so as to minimize the expected error in the site-specific q-value. This is achieved when the weighting factor is given by the ratio of the variance of the distribution of true q-values and the sum of the variances of true q-values and the variance of $q_{long} - q_{true}$, i.e., the squared uncertainty in q_{long}. If equal uncertainty in q_{long} is assumed for all sites, it is easy to calculate the weighting factor that should be used for all sites. The weighting factor is then the ratio between the squared variability expected on the basis of the variations in the CSA (0.06^2 at 13.0 T observed in this study) and the square of the standard deviation of the experimentally determined q_{long}-values. When this approach was used to analyze the ribonuclease H relaxation data for exchange broadening, the approach using weighted q-values yielded approximately 10% more precise exchange terms from the 500 and 600 MHz data than when q_{long} was used as a measure of q in eq 8, as in the original publication.[3]

E. How Does the Variability in the CSA Parameters Affect TROSY? Variability in the orientation and magnitude of the shielding tensor has an impact on the TROSY approach,[2] where the narrow component in the doublet is observed selectively. The optimal TROSY field has received attention previously.[38] Here the impact of the variations in the CSA tensors is assessed. The natural width of the narrow component is given by $2(R_2 - \eta_{xy})$,[17] preferably in rad s^{-1}. At a certain optimal magnetic field the CSA and dipole−dipole relaxation mechanisms cancel each other, to some degree, so as to produce the narrowest lines possible measured in ppm. The full width at half-height of the TROSY component measured in ppm, Δ^{TROSY}, is given as

$$\Delta^{TROSY} = 2(R_2 - \eta_{xy})/|\gamma_N B_0|\ 10^6 \qquad (11)$$

For a large macromolecule the spectral densities at the zero- and double-quantum frequencies can be neglected, so that $R_2 \approx (3d^2 + 4c^2)/24(4J(0) + 3J(\omega_N))$. The optimal field is evaluated by setting the first derivative of eq 11 with respect to B_0 equal to zero, with the expression for R_2 and η_{xy} (equation 1a) inserted, and solving for B_0. It is found that the field where optimal resolution in the nitrogen dimension of a TROSY spectrum is expected is given by the equation:

$$B_0 = \frac{\mu_0}{4\pi}\frac{3\gamma_H}{2}\frac{h}{2\pi}\frac{1}{\Delta\sigma_{eff}{r_{eff}}^3} \qquad (12)$$

For $\Delta\sigma_{eff} = 169$ ppm and $r_{eff} = 1.041$ Å, the optimal field is 22.2 T, corresponding to a 945 MHz proton resonance frequency. The variability of magnitudes of the shielding anisotropies is approximately 5.3 ppm. The optimal field is consequently expected to fall in the range between 21.5 and 22.9 T (920 and 980 MHz proton resonance frequency) for approximately two-thirds of the nitrogen atoms. The line width (in ppm) as a function of the magnetic field decreases relatively steeply until the minimum is reached (Figure 10). At higher fields the line width increases less steeply, thus the broadest lines in the TROSY spectrum are expected to be less broad at a somewhat higher field than 945 MHz.

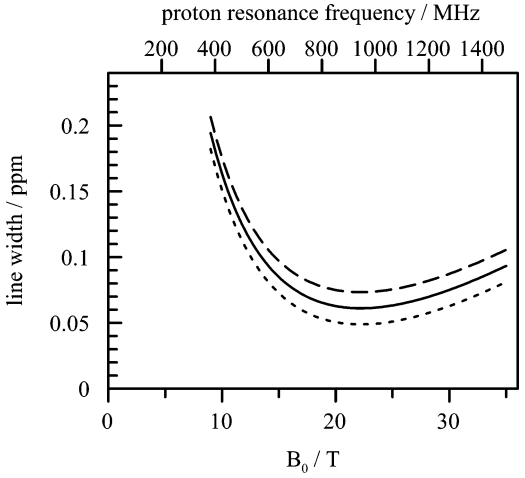

Figure 10. Graph illustrates the expected natural line width, in ppm, of the narrow component in the ^{15}N-doublet as a function of the magnetic field. The solid curve represents $f_{orient} = -0.80$, the dashed curve, $f_{orient} = -0.76$, and the dotted curve, $f_{orient} = -0.84$. The parameters $\Delta\sigma_{eff} = 169$ ppm, $r_{eff} = 1.041$ Å, and $\tau_c = 50$ ns were used for all curves.

The orientation factor determines how well the two mechanisms cancel each other (Figure 10). It is found that at the optimal magnetic field the line width is proportional to $1 + f_{orient}$. With an average f_{orient} of −0.80 and a variability of 0.04, some variations in the performance of the nitrogen TROSY along the polypeptide backbone are expected due to variations in the orientation of the shielding tensor. If additional relaxation mechanisms are active, optimal resolution is achieved at a different field, and the TROSY approach becomes less successful.

Concluding Remark

In conclusion, we find limited, yet statistically significant, variations in the magnitude and orientation of the chemical shift anisotropy tensors of the nitrogen atoms along the polypeptide backbone in ubiquitin. The effects of the variations are important for precise interpretation of protein dynamics from NMR relaxation studies at high magnetic field and for the evaluation of conformational exchange broadening.

Acknowledgment. This study was supported by a grant from the Swedish Research Council and by the European Commission, Contracts HPRN-CT-2001-00242 and QLK3-CT-2002-01989. The Swedish NMR center is acknowledged for use of their NMR spectrometers.

Supporting Information Available: Four tables containing the experimental relaxation rates from 9.39, 11.7, and 18.8 T, one table containing the fitted CSA parameters, $\Delta\sigma_{eff}$ and f_{orient}, one table showing the average q-values for each residue type, a description of the consistency test that was used, and three graphs where the isotropic nitrogen shifts are correlated to q(13 T), $\Delta\sigma_{eff}$, and CSA_g. This material is available free of charge via the Internet at http://pubs.acs.org.

JA045956E

(38) Pervushin, K. *Q. Rev. Biophys.* **2000**, *33*, 161−97.